

The transmembrane protein p23 contributes to the organization of the Golgi apparatus

Manuel Rojo^{1,*}, Gregory Emery¹, Varpu Marjomäki², Alasdair W. McDowall³, Robert G. Parton³ and Jean Gruenberg^{1,†}

¹Department of Biochemistry, University of Geneva, 1211 Genève 4, Switzerland

²University of Jyväskylä, Department of Biological & Environmental Science, 40351 Jyväskylä, Finland

³Centre for Microscopy & Microanalysis, Centre for Molecular & Cellular Biology and Department of Physiology & Pharmacology, University of Queensland, 4072 Brisbane, Australia

*Present address: U523 – Institut de Myologie, Groupe Hospitalier Pitié-Salpêtrière, 75651 Paris Cedex 13, France

†Author for correspondence (e-mail: jean.gruenberg@biochem.unige.ch)

Accepted 20 December 1999; published on WWW 21 February 2000

SUMMARY

In previous studies we have shown that p23, a member of the p24-family of small transmembrane proteins, is highly abundant in membranes of the cis-Golgi network (CGN), and is involved in sorting/trafficking in the early secretory pathway. In the present study, we have further investigated the role of p23 after ectopic expression. We found that ectopically expressed p23 folded and oligomerized properly, even after overexpression. However, in contrast to endogenous p23, exogenous p23 molecules did not localize to the CGN, but induced a significant expansion of characteristic smooth ER membranes, where they accumulated in high amounts. This ER-derived, p23-rich subdomain displayed a highly regular morphology, consisting of tubules and/or cisternae of constant diameter, which were reminiscent of the CGN membranes containing

p23 in control cells. The expression of exogenous p23 also led to the specific relocalization of endogenous p23, but not of other proteins, to these specialized ER-derived membranes. Relocalization of p23 modified the ultrastructure of the CGN and Golgi membranes, but did not affect anterograde and retrograde transport reactions to any significant extent. We conclude (i) that p23 has a morphogenic activity that contributes to the morphology of CGN-membranes; and (ii) that the presence of p23 in the CGN is necessary for the proper organization of the Golgi apparatus.

Key words: Membrane domain, Biosynthetic pathway, p24 protein family, Morphogenesis, Protein sorting

INTRODUCTION

Recently, a new family of transmembrane proteins has been discovered in animals, fungi and plants (the p24-family: Stamnes et al., 1995; Emery et al., 1999). Although their precise functions remain unclear or controversial, experimental evidence implicates some members of this family in protein sorting and transport in the secretory pathway. Yeast null mutants of the p24 proteins EMP24 and/or ERV25 secrete a subset of proteins with delayed kinetics when compared to wild-type yeast cells (Schimmöller et al., 1995; Belden and Barlowe, 1996), and yeast cells devoid of emp24p are deficient in the retention of ER-resident proteins (Elrod-Erickson and Kaiser, 1996). In mammalian cells, microinjected antibodies against the cytoplasmic tail of p23 inhibit the transport of cargo molecules (Rojo et al., 1997b; Majoul et al., 1998).

In agreement with a role in secretion, some p24 proteins have been localized to the interface between ER and Golgi: yeast erv25p to the ER (Belden and Barlowe, 1996), mammalian p23 and p24 to the cis-Golgi network (CGN: Rojo et al., 1997b; Blum et al., 1999), and mammalian gmp25 to the

smooth ER and to the CGN (Dominguez et al., 1998). Transport between ER and Golgi is mediated by coated vesicles (COPI and COPII: reviewed by Kuehn and Schekman, 1997; Cosson and Letourneur, 1997). Several members of the p24 family display anterograde and retrograde transport determinants in their transmembrane and cytoplasmic domains (Fiedler et al., 1996, 1997; Nickel et al., 1997; Nakamura et al., 1998), and peptides equivalent to the cytoplasmic tails of some p24 proteins are able to interact with COPI and/or COPII proteins in vitro, albeit with different specificities and affinities (Fiedler et al., 1996; Sohn et al., 1996; Dominguez et al., 1998). Therefore, it was inferred that the cytoplasmic tails of p24 proteins mediate their loading into COPI and/or COPII vesicles in vivo. It was also found that several p24 proteins partition into COP coated vesicles generated in vitro: COPI in mammals (Stamnes et al., 1995; Sohn et al., 1996) and COPII in yeast (Schimmöller et al., 1995; Belden and Barlowe, 1996), suggesting that some p24 proteins may act as coat receptors on transport vesicles (p23: Sohn et al., 1996).

The phenotype of yeast null mutants of EMP24 and ERV25 (see above) suggests that emp24p and erv25p participate in

cargo selection. The presence of yeast p24 proteins on COPII coated vesicles generated in vitro led to the proposal that they may act as cargo adaptors, and specifically interact with cargo molecules on transport vesicles (Schimmöller et al., 1995; Belden and Barlowe, 1996). Until now, no specific association between a p24 protein and a cargo molecule has been reported. However, it is possible that p24-cargo interactions are weak and/or transient, and cannot be revealed by classical biochemical approaches. Alternatively, it is possible that p24 proteins do not directly interact with cargo molecules, and that they participate in cargo selection by contributing to organelle structure (Elrod-Erickson and Kaiser, 1996).

In previous studies, we have investigated the role of p23 in mammalian cells (Rojo et al., 1997b). Our data indicated that p23 is unlikely to provide the major COP binding sites on biosynthetic membranes, since it was not enriched in COPI-coated vesicles generated in vitro, when compared to total p23-containing membranes, and since membrane-association of COPI in vitro was independent of p23. We found that p23 is a major component of the CGN, accounting for ≈30% of all integral membrane proteins. This together with our observations that divalent antibodies, but not Fab fragments, inhibited transport lead us to propose that p23-rich membranes contribute to CGN structure (Rojo et al., 1997b).

Here, we demonstrate that p23 is morphogenic. Overexpressed p23 molecules are retained within specialized membrane subdomains, which are continuous with the ER, at least dynamically. These membranes exhibit a highly regular and flat morphology reminiscent of the p23-rich membranes and of Golgi cisternae. Upon overexpression, endogenous p23, but not other CGN and Golgi proteins, becomes selectively relocalized from the CGN to the membrane domains containing ectopically expressed p23 molecules. This expression-dependent p23 depletion caused alterations of the CGN and Golgi complex organization, indicating that p23 molecules participate in the biogenesis and/or maintenance of CGN and Golgi apparatus organization.

MATERIALS AND METHODS

Reagents, antibodies and standard methods

Cycloheximide, brefeldin A (BFA), and tunicamycin were from Sigma Chemical Co. (St Louis, MO); stock solutions (cycloheximide: 10 mg/ml in water; BFA: 5 mg/ml in methanol; tunicamycin: 5 mg/ml in DMSO) were kept at -20°C. Endoglycosidase H (endo H) was from Boehringer Mannheim. The FITC-labeled B subunit of verotoxin 1 (VTB: Kim et al., 1996), and a KDEL-bearing B-fragment of Shiga toxin (STB: Johannes et al., 1997) were kindly provided by C. Lingwood (Hospital for Sick Children, Toronto, Canada) and L. Johannes (Institute Curie, Paris, France), respectively. STB was labeled with Cy3.5 (FluoroLink reactive dye, Amersham) following the instructions of the manufacturer. Anti-peptide antibodies specific for p23 have been described (Rojo et al., 1997b). Antibodies against the luminal domain of p23 were generated in rabbits. Rabbit antisera against calnexin (Hammond and Helenius, 1994), the mammalian KDEL-receptor ERD2 (Griffiths et al., 1994), and mammalian sec13p (Tang et al., 1997) were kind gifts from A. Helenius (Swiss Federal Institute of Technology, Zürich, Switzerland), H. D. Söling (University of Göttingen, Göttingen, Germany), and B. L. Tang (University of Singapore, Singapore), respectively. Mouse mAb against mannosidase II (53FC3: Burke et al., 1982), β'-COP (CM1A10: Orci et al., 1993), giantin (Linstedt and Hauri, 1993), and

two Golgi antigens (CTR314 and CTR433: Jasmin et al., 1989) were kindly provided by B. Burke (University of Calgary, Canada), F. Wieland (University of Heidelberg, Heidelberg, Germany), H. P. Hauri (University of Basel, Basel, Switzerland), and M. Bornens (Institute Curie, Paris, France), respectively. A mouse mAb against the C-terminal peptide of grp78/BiP was obtained from StressGen Biotechnologies Corp. (Victoria, Canada). Polyclonal antibodies against VSV (Gruenberg and Howell, 1985), mouse mAbs that recognize the myc epitope (9E10: Evan et al., 1985), a cytoplasmic epitope of VSV-G (P5D4: Kreis, 1986), and an exoplasmic epitope of VSV-G (17.2.21.4: Gruenberg and Howell, 1985) have been described. Fluorescein-labeled anti-mouse IgG, rhodamine-labeled anti-rabbit IgG, and fluorescein-labeled streptavidin were from Jackson ImmunoResearch Laboratories, Inc. (West Grove, PA). Protein analysis (protein determination, SDS-PAGE and western blot) was performed as described (Rojo et al., 1997b).

Cloning and cDNAs

The complete open reading frame of the BHKp23 cDNA (accession number AJ001513) was amplified by PCR from pBSK-BHKp23 with a T3 forward primer (5'-AAT TAA CCC TCA CTA AAG GG-3') and a reverse primer containing a flanking *Bam*HI site (5'-CGC GGA TCC TCA TTA CTC TAT CAA CTT C-3', *Bam*HI site in bold). The PCR-product was digested with *Eco*RI and *Bam*HI, and cloned into the pBSK vector (Stratagene). A myc-tagged p23 molecule was constructed by fusing the myc-epitope to the N terminus of the mature polypeptide. To this end, the cDNAs coding for the signal sequence (positions 31 to 123) and the mature polypeptide (positions 124-690) were amplified separately. The DNA coding for the signal peptide was amplified with the T3 forward primer and with a reverse primer coding for a glycine residue, the myc epitope EQKLISEEDL, and a *Bg*III site (5'-TAA GAT CTT CTT CTG AGA TTA GTT TTT GTT CGC CGG CGA GCA CCG AGC TGG GGC-3', myc-coding sequence underlined, *Bg*III site in bold). The cDNA coding for the mature peptide was amplified with a forward primer containing a flanking *Bg*III site (5'-GAA GAT CTT ATC TCC TTC CAT CTG CCC G-3', *Bg*III site in bold) and with the reverse primer containing a flanking *Bam*HI site. Both PCR fragments were digested with *Bg*III, ligated to mycp23, digested with *Eco*RI/*Bam*HI, and cloned into the pBSK vector. The cDNA coding for the mature luminal domain of p23 was amplified by PCR with forward and reverse primers containing flanking *Nco*I and *Bam*HI-sites, respectively. The PCR-product was digested with *Nco*I and *Bam*HI, and cloned into the pET15B-vector (Novagen). The 6His-tagged luminal domain of p23 was expressed in *Escherichia coli* and purified with Ni-agarose as described by the manufacturer (Novagen). All PCR-products (30 cycles; Pfu polymerase, Stratagene) were verified by DNA sequencing. The cDNAs coding for p23 and mycp23 were cloned into the expression vectors pCB6 (Brewer, 1994), pSFV1 (Liljestrom and Garoff, 1991), and pIND (Invitrogen). The pCB6 and pSFV vectors were kindly provided by Karl Matter (University of Geneva, Switzerland) and Henrik Garoff (Karolinska Institute, Huddinge, Sweden), respectively. The cDNAs coding for the tsO45 mutant of the vesicular stomatitis virus (VSV) glycoprotein G (tsO45-G: Gallione and Rose, 1985), for a myc-tagged NAGTI-GFP chimera (Shima et al., 1997) and for myc-tagged ERD2 (mycERD2: Lewis et al., 1992) were kindly provided by K. Simons (European Molecular Biology Laboratory, Heidelberg, Germany), D. Shima and G. Warren (ICRF, London, UK) and M. Lewis (Laboratory of Molecular Biology, Cambridge, United Kingdom), respectively; tsO45-G and mycERD2 were cloned into the expression vectors pCB6 and pIND.

Cell culture, transfection, and virus infection

Monolayers of BHK and HeLa cells were maintained as described (Rojo et al., 1997b). A HeLa cell line harboring a chimera consisting of an enhanced green fluorescent protein (GFP) fused to the retention domain of *N*-acetylglucosaminyl-transferase (mycNAGTI-GFP) was

kindly provided by D. Shima and G. Warren (ICRF, London, UK), and were maintained as described (Shima et al., 1997). When required, cells were incubated with 20 $\mu\text{g/ml}$ BFA, 20 $\mu\text{g/ml}$ cycloheximide, or 5 $\mu\text{g/ml}$ tunicamycin for the indicated periods of time. For short term (≤ 3 hours) incubations of cells at 15, 20 or 31°C, cell culture medium was replaced by MEM containing 10 mM Hepes, pH 7.4, and 5 mM glucose. Cells were incubated with VTB or STB ($\approx 10 \mu\text{g/ml}$ in PBS) at 0°C for 1 hour, and cells were then transferred to complete MEM and incubated at a 37°C for the indicated times. Cells were transfected with the calcium phosphate technique (Chen and Okayama, 1987), and analyzed 36–48 hours after addition of DNA. In co-transfection experiments with pCB6-p23 and pIND-tsO45-G, cells were transferred to a 40°C incubator and tso45-G expression was induced (by addition of 1 μM muristerone A) 24 hours after DNA addition. Recombinant SFV virions (expressing SFV-p23 or SFV-mycp23) were produced as described (Liljestrom and Garoff, 1991). Cells were infected with VSVtsO45 (Indiana Serotype) or recombinant SFV as described (Kreis et al., 1986; Liljestrom and Garoff, 1991). For double infection, cells were simultaneously incubated with both VSVtsO45 and SFV-mycp23. The acquisition of endo H resistance by ^{35}S -Met labelled tsO45-G was measured as described (Balch et al., 1986). The tsO45-molecules at the plasma membrane of non-permeabilized cells were detected with antibodies against the luminal domain of VSV-G (Rojo et al., 1997b). The fluorescence of ≥ 50 cells was quantified on a cell-to-cell basis, and this accounted for and compensated cell to cell variations within a sample.

Membrane solubilization and gel filtration

Microsomal membranes were collected by sedimentation (TLS-55, 55000 rpm, 30 minutes) from post-nuclear supernatants of homogenized BHK or HeLa cells (Rojo et al., 1997b). Membranes were resuspended by repeated pipetting in solubilization medium (20 mM Tris-HCl, pH 7.4, 0.2 mM EDTA, 150 mM Na_2SO_4 or NaCl) devoid of detergent (final protein concentration 5 mg/ml). Detergent concentration was then adjusted to 3% (w/v) by addition from a 20% stock in water. Membranes were solubilized by repeated pipetting for 5 minutes at room temperature, and insoluble material was removed by centrifugation (4 minutes, 30 psi $\approx 135000 \text{ g}$, $k=11$) in a Beckman Airfuge (Rojo and Wallimann, 1994; Rojo et al., 1997a).

Aliquots (50 μl) of the supernatant were applied to a superose 12 PC 3.2/3.0 column, and the column was eluted at 50 $\mu\text{l/minute}$ (SMART system, PHARMACIA) with solubilization medium containing the indicated detergent (Triton X-100 (TX100) or Na-cholate: 0.5%; octyl-polyoxyethylene (8POE): 1%). Fractions were subjected to protein precipitation with chloroform/methanol (Wessel and Flügge, 1984) and analyzed by SDS-PAGE and western blot. The column was calibrated with soluble proteins of known molecular mass and Stokes radius (kDa/nm): RNase A (14/1.64), BSA (67/3.55), aldolase (158/4.81), IgG (180/5.1), catalase (232/5.22), ferritin (440/6.1), thyroglobulin (669/8.5). The elution profile of these proteins was identical in the presence and absence of 8POE.

The molecular mass of p23 solubilized in 8POE was estimated with the exponential fit shown in Fig. 2D and assuming that: (1) the size of mixed protein-detergent micelles is overestimated by 10–20% when using soluble proteins for calibration (le Maire et al., 1986), (2) the mean molecular mass of 8POE-micelles is 22750 Da (monomeric 8POE: 350 Da; aggregation number of pure 8POE-micelles: 65 ± 4 ; Zulauf et al., 1985), and (3) the number of detergent molecules in a mixed protein-detergent micelle is lower (down to 40%) or equal than that of pure detergent micelles (le Maire et al., 1983, and references therein).

Immunofluorescence and electron microscopy

Cells were processed for immunofluorescence as described (Rojo et al., 1997b). Immunofluorescence images were acquired, processed and analyzed as described by Rojo et al. (1997b). For electron microscopy, cells were fixed with 8% paraformaldehyde in 250 mM

Hepes, pH 7.4, for ≥ 1 hour, washed with PBS, incubated with 50 mM NH_4Cl , and scraped with a rubber policeman. Cells were sedimented, gently resuspended in 10% warm gelatin in PBS, and further processed for cryosections and immunogold labeling as described (Griffiths et al., 1984). In some experiments (e.g. Fig. 4D–F) sections were retrieved using a methylcellulose/sucrose mixture as described by Liou et al. (1997).

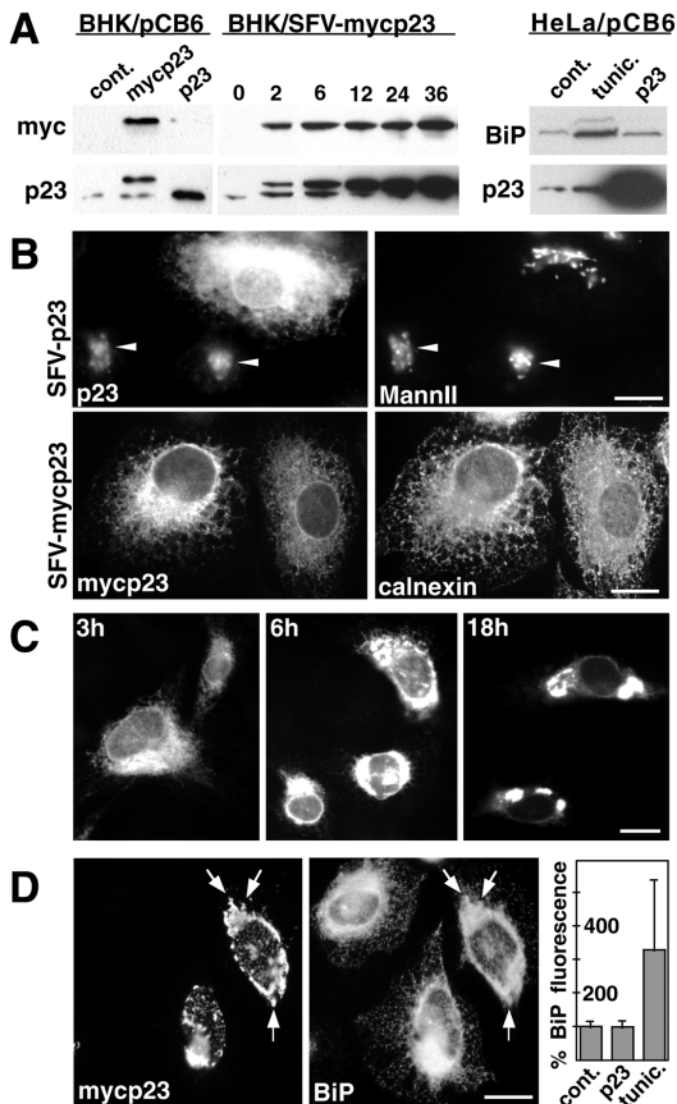
RESULTS

Ectopically-expressed p23 forms large membrane domains in continuity with the ER

Upon overexpression, the p23 protein was processed to the same apparent molecular mass as the endogenous protein (Fig. 1A: BHK/pCB6), demonstrating that the signal peptide had been cleaved by the signal peptidase in the lumen of the ER. For convenient detection, we also engineered a p23 protein tagged with a myc-epitope (mycp23). Because the cytoplasmic tails of transmembrane proteins are relevant for proper function and localization (Kirchhausen et al., 1997), the myc-tag was placed near the N terminus, directly after the predicted cleavage site of the signal peptidase (see Materials and Methods). As predicted, myc-tagged p23 molecules could be detected with antibodies against the myc epitope (Fig. 1A: myc), and their apparent molecular mass was higher than that of endogenous p23 (Fig. 1A: mycp23).

When overexpression of p23 was driven by the cytomegalovirus (CMV) promoter (the promoter present in the pCB6 expression vector, see Materials and Methods), the exogenous p23-molecules formed large compact structures that did not resemble any known biosynthetic or endocytic compartment when analyzed by immunofluorescence (see below Figs 1D, 3, 5C, 6B, 7A). We inferred that this may result from high level expression, and we expressed p23 with systems that allow protein expression at significantly lower levels: recombinant Semliki Forest virus (SFV: Fig. 1A and B) and expression vectors with an inducible promoter (pIND: Fig. 1C). Recombinant SFV infected 80–100% of the cells (not shown), allowing comparison of the levels of endogenous and exogenous p23 molecules by western blot analysis of total cell homogenates (Fig. 1A: BHK/SFV-mycp23). First, exogenous p23 was expressed to levels similar to those of endogenous p23: BHK cells were infected with SFV-p23 or SFV-mycp23 for 3 hours (cf. Fig. 1A), protein synthesis was then blocked by addition of cycloheximide for an additional 3h period, and cells were processed for immunofluorescence. Exogenous p23 (both wild-type and myc-tagged) distributed to an extensive reticular membrane system and largely colocalized with calnexin, a transmembrane marker of the ER (Fig. 1B). With increasing levels of expression, p23 molecules formed large compact structures (Fig. 1C, up to several μm) that resembled those observed upon transfection of cells with CMV-based vectors (Figs 1D, 3, 5C, 6B and 7A).

The localization of exogenous p23 molecules to the ER and the formation of large membrane clusters were somewhat unexpected, as the endogenous p23 localizes to the CGN at steady state (Rojo et al., 1997b). Therefore, we investigated whether the behaviour of exogenous p23 molecules was due to protein misfolding. Eukaryotic cells respond to the accumulation of unfolded proteins in the ER by increasing the



transcription of genes encoding ER chaperones like BiP/grp78 or grp94 (Kozutsumi et al., 1988). Here, we investigated whether the levels of BiP/grp78 increased upon overexpression of p23. Localization of BiP by immunofluorescence revealed that p23-clusters were accessible to BiP (Fig. 1D, arrows), confirming that p23-clusters remain continuous with the ER. western blot analysis of cell homogenates (Fig. 1A) and quantitative immunofluorescence of cells (Fig. 1D) demonstrated that retention of overexpressed p23 molecules in the ER did not increase the cellular level of BiP/grp78. In contrast, the levels of both BiP/grp78 and grp94 (Fig. 1A,D) increased upon induction of the unfolded protein response with the glycosylation inhibitor tunicamycin (Kozutsumi et al., 1988). Altogether, this indicates that retention of exogenous p23 in the ER is not due to misfolding of p23.

Endogenous and exogenous p23 molecules assemble into oligomeric complexes

Since all p24 proteins display heptad repeats of hydrophobic aminoacids that are suited for coil-coiled interactions, it was proposed that p24 proteins interact with each other and/or oligomerize (Stamnes et al., 1995; Emery et al., 1999). Indeed,

Fig. 1. Ectopically expressed p23 molecules are retained in the ER. BHK (A-C) or HeLa cells (A,D) were transfected with pCB6-p23, pCB6-mycp23 (A,D), pIND-mycp23 (C), or infected with SFV-mycp23 (A,B). Overexpression of exogenous molecules occurs in $\leq 5\%$ (BHK) or $\geq 50\%$ (HeLa) of cells subjected to transfection, and in 80-100% of BHK cells subjected to SFV-infection. (A) Transfected (pCB6) or infected cells (SFV-mycp23) were homogenized, processed for western blot and analyzed with antibodies against p23 (p23), the c-Myc epitope (myc), or BiP/grp78 (BiP). The antibody against the c-terminal peptide of BiP decorates BiP/grp78 and grp94. Cell homogenates were processed for western blot 48 hours after DNA addition (pCB6) or at the indicated times (hours) after infection (SFV-mycp23). Exogenous and endogenous p23 molecules are processed to the same apparent molecular mass. The increased apparent molecular mass of mycp23 results from the presence of the c-Myc epitope. The levels of BiP/grp78 and grp94 increase when the unfolded protein response is induced with tunicamycin (HeLa, tunic.), but not upon overexpression of p23 in $\geq 50\%$ of cells (HeLa, p23). (B) BHK cells were infected with viruses coding for p23 proteins. Cycloheximide was added 3 hours after infection, and after further 3 hours cells were processed for immunofluorescence. Endogenous p23 distributes to the perinuclear Golgi region, where it colocalizes with mannosidase II (SFV-p23: arrowheads). Exogenous p23 molecules localize to the ER, where they colocalize with calnexin (SFV-mycp23). (C) BHK cells were transfected with pIND-mycp23, and 36 hours post-transfection the expression of p23 was induced for the indicated times. Ectopically expressed p23 molecules cluster in the ER. (D) HeLa cells transfected with pCB6-mycp23 were processed for immunofluorescence with the indicated antibodies. BiP partially distributes to clusters of p23 molecules (arrows). For each condition (control, p23, tunic.) the mean BiP fluorescence/cell area of ≥ 50 cells was quantified and expressed as % of the mean BiP fluorescence in control cells. BiP fluorescence was not increased upon overexpression of p23 (p23), but upon treatment of cells with tunicamycin (tunic.). Bars, 5 μm .

cross-linking studies in yeast indicate that different p24 proteins interact with each other (Belden and Barlowe, 1996), and density gradient centrifugation of detergent treated membranes revealed the presence of large oligomeric complexes (Dominguez et al., 1998). Here we investigated the size and oligomeric structure of solubilized, endogeneous p23 by gel chromatography.

Since solubilization conditions largely determine the conformation, structure, and activity of solubilized membrane proteins, it is thus necessary to establish conditions which maintain a particular integral membrane protein in its native form (Hjelmeland and Chrambach, 1984; Rojo and Wallimann, 1994). Here, p23 was solubilized with the 'milder' detergents TX100, 8POE, and sodium cholate (cholate), to avoid the monomerization and/or denaturation that can be induced by 'harsher' detergents (e.g. SDS). To investigate the influence of the ionic strength, solubilization was performed with buffers containing 150 mM of either NaCl or Na₂SO₄ (Rojo, 1993).

After solubilization, insoluble material was removed by centrifugation and solubilized proteins were analyzed by SDS gel electrophoresis and western blotting. Whereas p23 solubilization was quantitative and independent of the ionic strength with both TX100 and 8POE (Fig. 2A), solubilization with cholate was only partial, and required the higher ionic strength of the Na₂SO₄-containing buffer (Fig. 2A). In the presence of TX100 or 8POE, an analysis of the supernatants by gel filtration (using Na₂SO₄) showed that p23 molecules

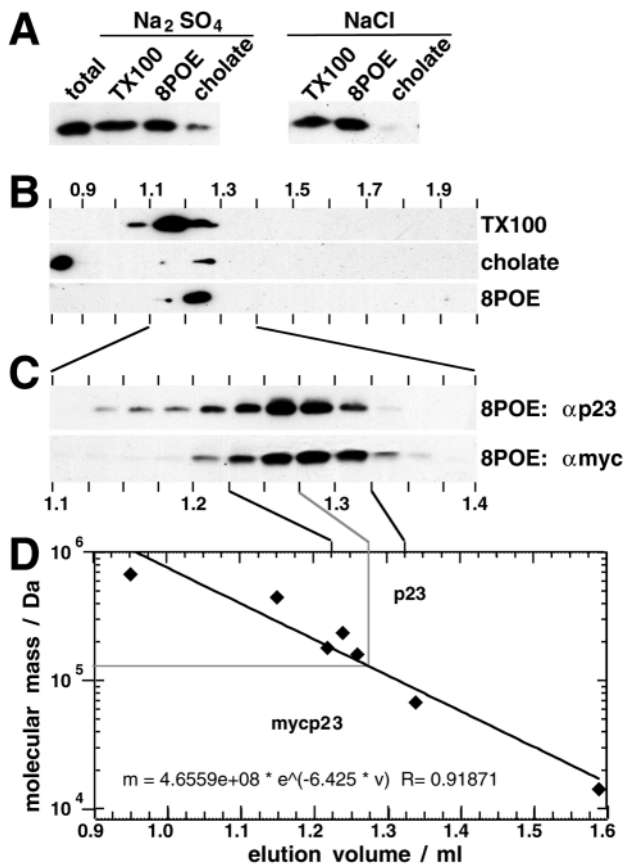


Fig. 2. Endogenous and exogenous p23 molecules assemble into oligomeric complexes. (A) BHK microsomes were subjected to detergent solubilization under the indicated conditions. Insoluble material was removed by centrifugation and supernatants were analyzed by SDS gel electrophoresis and western blotting using antibodies against p23. With TX100 and 8POE, the solubilization was quantitative, and independent of the ionic strength. With cholate, solubilization was only partial, and required the higher ionic strength of the Na₂SO₄-containing buffer. (B) Supernatants were fractionated using a Superose 12 column, and fractions were analyzed for p23 as above. With TX100 and 8POE, all p23 molecules eluted in a monodisperse peak. With cholate, most p23 molecules eluted in the void volume, and a significantly minor fraction eluted later. (C) Microsomes of control (αp23) or SFV-mycp23 (αmyc) infected cells were treated with 8POE and centrifuged. Supernatants were chromatographed with a Superose 12 column and 25 μl fractions were analyzed as in B with antibodies against p23 (αp23) or the myc tag (αmyc). The majority of endogenous and exogenous (myc-tagged) p23 molecules eluted between 1.225 and 1.325 ml (solid lines). The medial line of these fractions (the peak) was at 1.275 ml (grey line). (D) The superose 12 column was calibrated with soluble proteins of known molecular mass; the relationship between molecular mass and elution volume was fitted to the displayed exponential equation. According to this equation, the mean molecular mass of mixed p23-8POE micelles is 129 kDa. The size of the protein-moiety of these micelles corresponds to 80-107 kDa (see Materials and Methods), indicating that solubilized p23 exists as a tetramer.

then eluted as a monodisperse peak (Fig. 2B). With cholate, however, most p23 molecules eluted in the void volume ($\geq 2 \times 10^6$ Da, Fig. 2B); these molecules probably correspond to

partially solubilized (or aggregated) material, since they were only observed under conditions of partial solubilization (Fig. 2A: Na₂SO₄: cholate). With cholate, however, some p23 was also recovered in an elution volume comparable to that observed with TX100 and 8POE (Fig. 2B). This second cholate peak contained p23 molecules which had been solubilized despite these 'mild' conditions (Fig. 2A, cholate), and thus presumably corresponded to a protein complex preserved during solubilization.

We then used 8POE to estimate the size of p23 complexes after solubilization. Indeed, the small size of 8POE micelles (22750 Da) makes it possible to estimate the size of a protein in mixed 8POE micelles (see Materials and Methods). After calibration with soluble proteins of known sizes, and fitting the relationship between molecular mass and elution volume to an exponential equation, we calculated the size of p23-8POE micelles to be 129 kDa (Fig. 2C and D). From this value, we determined that the protein-moiety of the 8POE mixed micelles was 80-107 kDa (see Materials and Methods). Since the predicted molecular mass of p23 is 21.7 kDa (Rojo et al., 1997b), it is highly likely that p23 exists as a tetramer. We then compared this value with the size of complexes formed by ectopically expressed myc-tagged p23. BHK cells were infected with SFV-mycp23 for 4 hours, and microsomes were prepared and solubilized with 8POE. Analysis of superose 12 fractions with antibodies against the myc-epitope revealed an elution profile that was highly similar to that of endogenous p23 (Fig. 2C). These observations demonstrate that ectopically-expressed p23 oligomerizes properly, like the native endogeneous protein, confirming our findings that proper folding has occurred.

The overexpression of p23 leads to the specific relocation of endogenous p23

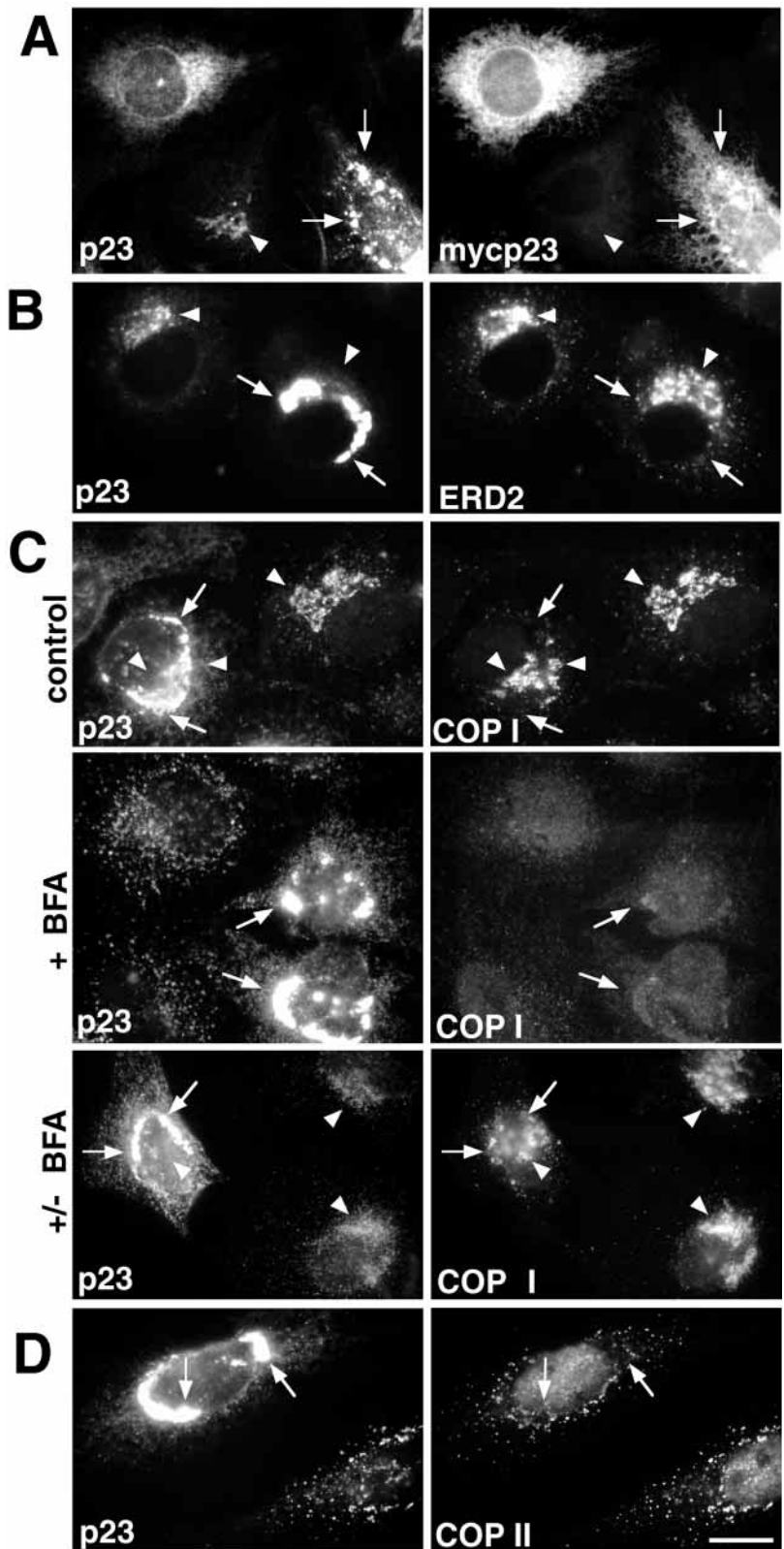
In order to characterize better the site where exogenous p23 molecules accumulated, we investigated the distribution of transmembrane markers of other intracellular compartments. In cells overexpressing p23, the ER marker calnexin distributed both to the ER and to p23 clusters, but (similarly to BiP) calnexin was not enriched in p23 clusters (not shown). The behaviour of calnexin and BiP indicates that p23-membranes remain continuous, at least dynamically, with the ER. The continuity of p23-clusters with the ER and their position within the biosynthetic pathway was further confirmed by electron microscopy (see below Fig. 4), and by the trafficking properties of the tsO45-G protein, which could enter and exit p23-clusters (see below: Fig. 5). The absence of ribosomes on these membranes (see below: Fig. 4) indicated that they probably represent subdomains of the smooth ER. The nature of p23-membranes was further investigated by centrifugation in a step sucrose gradient (Rojo et al., 1997b): the distribution of membranes containing exogenous p23 was similar to that of p23 membranes of the CGN, and different from that of ER-membranes (not shown). These observations confirmed that membranes containing exogenous p23 represent a specialized subdomain of the ER whose physical properties were largely determined by the abundance of p23 molecules.

Interestingly, the overexpression of exogenous p23 molecules led to the quantitative relocation of endogenous p23 molecules from the CGN (Fig. 3A: arrowhead) to the ER and to p23-clusters (Fig. 3A: arrows, and see below). Although

Fig. 3. Overexpression of p23 leads to the redistribution of endogenous p23 from the CGN to clusters of exogenous p23 molecules. (A) Transfected BHK cells expressing different levels of mycp23. In cells that do not express exogenous mycp23, endogenous p23 molecules localize to the CGN in the perinuclear Golgi region (arrowhead). In cells expressing exogenous mycp23, endogenous p23 relocates to the ER or ER clusters (arrows). (B-D) In non-transfected cells p23, ERD2 and COPI codistribute to the perinuclear Golgi region (arrowheads). In cells overexpressing p23, endogenous p23 is quantitatively relocated to ER clusters of exogenous p23-molecules (arrows). ERD2 (B), COPI (C), and COPII (D) do not relocate to p23-clusters. (C) The presence of p23 clusters does not modify the dynamics of COPI upon addition of BFA (+ BFA). Following removal of BFA (+/- BFA), COP I associates to biosynthetic membranes (arrowheads), but not to p23 clusters (arrows). Bars, 5 μ m.

some p23, below detection level, may remain in the IC/CGN after overexpression, these observations suggest that the bulk of p23 was redistributed under these conditions. In contrast, the KDEL receptor ERD2 which normally codistributes with p23 in the CGN (Fig. 3B: arrowhead; Rojo et al., 1997b), was not relocated to the clusters containing exogenous p23 (Fig. 3B: arrows). Neither were gp74 (Alcalde et al., 1994: not shown), and two members of the p24 family (T1/ST2: Gayle et al., 1996 and p26/ γ 4: Dominguez et al., 1998; G. Emery, M. Rojo and J. Gruenberg, unpublished). Therefore, relocation to the ER does not apply to all proteins of the CGN, nor to all members of the p24 protein family, and may be specific for p23. Several other transmembrane proteins of biosynthetic and endocytic membranes (mannosidase II, TGN38, transferrin receptor, LAMP1) were also absent from p23-clusters (not shown). However, the distribution of CGN and Golgi proteins was altered by p23 expression (see below: Fig. 7). The specific retention of endogenous and exogenous p23 molecules in the ER suggests (i) that p23 molecules constitutively cycle between the CGN and the ER, (ii) that endogenous and exogenous p23 molecules specifically interact with each other, and (iii) that endogenous and exogenous p23 have a similar structure.

We then investigated whether the intracellular distribution of COPI and COPII was altered after overexpression and relocation of p23. As shown in Fig. 2 (C: control and D), neither the COPI nor the COPII coat was relocated to clusters containing p23. To further investigate the possible role of p23 in the association of COP I to membranes, we used the drug brefeldin A (BFA). Addition of BFA led to a diffuse cytoplasmic staining of COPI, indicative of COPI solubilization, both in transfected and in non-transfected cells (Fig. 3C: +BFA). Subsequent removal of BFA led to reassociation of COP I to biosynthetic membranes, but not to membranes containing p23 molecules (Fig. 3C: +/- BFA).



Ectopically-expressed p23 forms an extensive tubulo-cisternal membrane system of highly uniform morphology

Immunoelectron microscopy of cryosections revealed that clusters of p23-molecules (labeled with antibodies against p23,

Fig. 4) consist of a large mass of smooth membranes with tubular appearance (Fig. 4). The size of the whole membrane complex, and the length of the tubular profiles (up to several μm , Fig. 4) was consistent with the size of the clusters observed by immunofluorescence. The immunofluorescence data (see above), the absence of ribosomes on these membranes and the possible presence of continuities between these membranes and the rough ER (see Fig. 4), suggests that these membranes are part of the smooth ER. Note that the rough ER, such as that surrounding the nucleus (Fig. 4A), showed negligible labeling for p23. The considerable length of these profiles in thin sections (Fig. 4) implies that they represent cross-sections of flat cisternae. The morphology of these membranes, with a narrow and uniform luminal space (Fig. 4, small arrowheads), is different from ER cisternae (which have a wider and more variable intermembrane distance; see for example the ER close to the nucleus in Fig. 4A), and reminiscent of endogenous p23-rich membranes in the CGN (Rojo et al., 1997b). As immunofluorescence had not revealed transmembrane markers of other compartments in p23 clusters (see above), we conclude that these membranes, and their particular morphology, were directly induced by the presence of p23 molecules. The morphogenic role of p23 in the formation of these structures is further supported by the high density of the protein in these membranes (see for example, Fig. 4B and C).

In order to investigate the structure of Golgi membranes in cells overexpressing p23, cells were co-transfected with expression plasmids encoding p23 as well as a myc- and GFP-tagged version of *N*-acetyl glucosamine transferase I (mycNAGTI-GFP), which localizes to the Golgi apparatus (Shima et al., 1997). The detection of mycNAGTI-GFP with anti-myc antibodies allowed the unambiguous identification of Golgi membranes in p23 overexpressing cells. Despite the high level of p23 labeling on tubules nearby, the Golgi stacks revealed negligible labeling for p23 (Fig. 4D and E), in agreement with our immunofluorescence experiments (Fig. 3B and C). In cells overexpressing p23, Golgi stacks retained their typical morphology (a series of apposed lamellae, Fig. 4D,E), but these stacks consistently appeared reduced in size when compared to control cells (transfected with NAGTI-GFP alone; Fig. 4F). These observations were further characterized by quantitative immunofluorescence (see below, Fig. 7).

Anterograde and retrograde transport in cells expressing exogenous p23

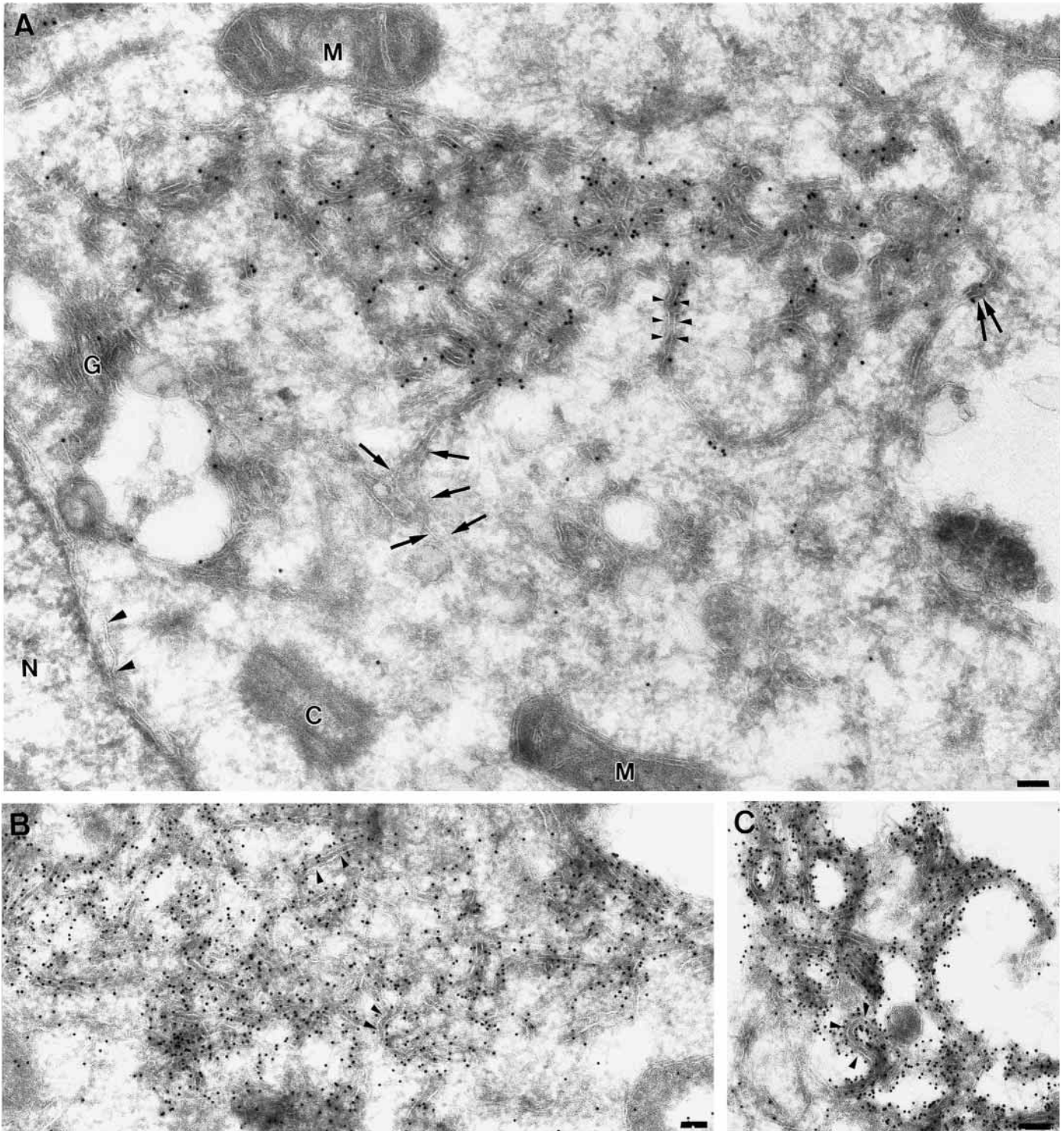
We previously observed that the p23 protein is a major component of the CGN (Rojo et al., 1997b), and that antibodies against the p23 cytoplasmic domain inhibit anterograde transport. We thus investigated whether the dominant negative effect of exogenous p23 on the localization of the endogenous p23 (see above), affected the transport capacity of a CGN that has been depleted from p23.

The tsO45-mutant of VSV-G (tsO45-G) remains misfolded in the ER at the restrictive temperature of 40°C, and is properly folded and transported to the plasma membrane at the permissive temperature of 31°C (Bergmann et al., 1981). Here, we investigated the anterograde transport of tsO45-G in control cells and in cells overexpressing p23. We used two methods for coexpression of p23 and tsO45-G that yielded identical results: cells were either simultaneously infected with the tsO45 mutant of VSV and with recombinant SFV coding for

mycp23 (SFV-mycp23) or doubly transfected with vectors for constitutive expression of p23 and for inducible expression of tsO45-G (pCB6-p23 and pIND-tsO45-G, see Materials and Methods). In both cases, the tsO45-G protein was expressed for 12 hours at 40°C, and cycloheximide was added to inhibit further protein synthesis. Then, cells were either fixed (Fig. 5A: 40°C), or incubated at different temperatures for varying periods of time (15 and 20°C for 3 hours, 31°C for 30 or 60 minutes) prior to fixation. At 40°C, the misfolded tsO45-G molecules localized to the ER in cells transfected/infected with tsO45-G alone, and to p23-clusters in 96% of cells ($n=105$) doubly transfected/infected with tsO45-G and p23 (Fig. 5A: 40°C). This confirmed that p23-clusters represent ER-subdomains which are continuous with the rough ER, at least dynamically. When the temperature was lowered to a permissive value (15°C and 20°C for 3 hours; 31°C for 30 or 60 minute), the tsO45-G protein folded properly and reached membranes that normally correspond to the intermediate compartment (Fig. 5A: 15°C), to the TGN (not shown: 20°C), to the Golgi complex (Fig. 5A: 31°C), and to the plasma membrane (Fig. 5C).

We then quantified the transport capacity of cells that overexpress and relocalize p23. As shown in Fig. 5B, transport of tsO45-G to the CGN (Fig. 5B), measured by acquisition of endoglycosidase H resistance (Balch et al., 1986), occurred with similar, albeit slower kinetics, when compared to control cells. This small, but significant, reduction in transport rates may have been caused by changes in Golgi organization (Fig. 4, and see below). Transport to the cell surface was measured by immunofluorescence in non-permeabilized cells (Fig. 5D) 1 hour after release of the temperature block. Anterograde transport of VSV-G from the ER to the plasma membrane was not significantly altered upon p23 depletion from the CGN (Fig. 5D: pINDtsO45). Minor changes, as those observed by endoH resistance, could not be detected by immunofluorescence.

Some bacterial toxins which bind cell surface receptors (verotoxins or shiga-like toxins) reach the ER after travelling through endosomes and Golgi complex, and they are assumed to travel along an endogenous pathway for retrograde transport (reviewed by Johannes and Goud, 1998). Here, we investigated the retrograde transport of the B subunit of verotoxin 1 (VTB; Kim et al., 1996). HeLa cells were incubated with FITC-labeled VTB at 4°C, and VTB was then internalized for increasing periods of time. Immunofluorescence confirmed that, after binding to the plasma membrane (Fig. 6A: 0 minutes; note the continuous labelling of cell edges and pseudopodia), VTB is efficiently transported to the Golgi apparatus (Fig. 6A: 30, 90 minutes; note the gradual disappearance of plasma membrane labeling). After longer incubations, VTB molecules were visualized in the Golgi region and in dispersed structures that correspond to the ER (Fig. 6A: 4 hours; note the absence of labelling on the cell edge). We then investigated whether overexpression and relocalization of p23 affected the retrograde transport of VTB. VTB molecules reached not only the ER, but also ER subdomains containing clusters of p23-molecules (Fig. 6B) in the vast majority of transfected cells (72%, $n=25$). Identical results were obtained with a shiga-toxin B subunit that had been appended with the KDEL retrieval peptide (STB; Johannes et al., 1997; not shown). We conclude from these



results that the presence of p23-domains in the CGN is not essential for the anterograde transport of a transmembrane cargo molecule (VSV-G) to the Golgi and to the plasma membrane, and for the retrograde transport of shiga-like toxins to the Golgi and to the ER.

Quantitative analysis of Golgi organization in cells overexpressing p23.

When overexpressed, p23 caused the appearance of an extensive

tubulo-cisternal membrane system of highly uniform morphology, in which the p23 protein accumulated (see Fig. 4A). At the ultrastructural level, we found that it was difficult to identify the Golgi apparatus in these cells, when compared to control cells. In appropriate sections, however, individual Golgi stacks were sometimes visible, but these appeared smaller than the Golgi apparatus in control cells (see above: Fig. 4). These observations suggested that the integrity of the Golgi ribbon had been affected, and thus, that overexpression

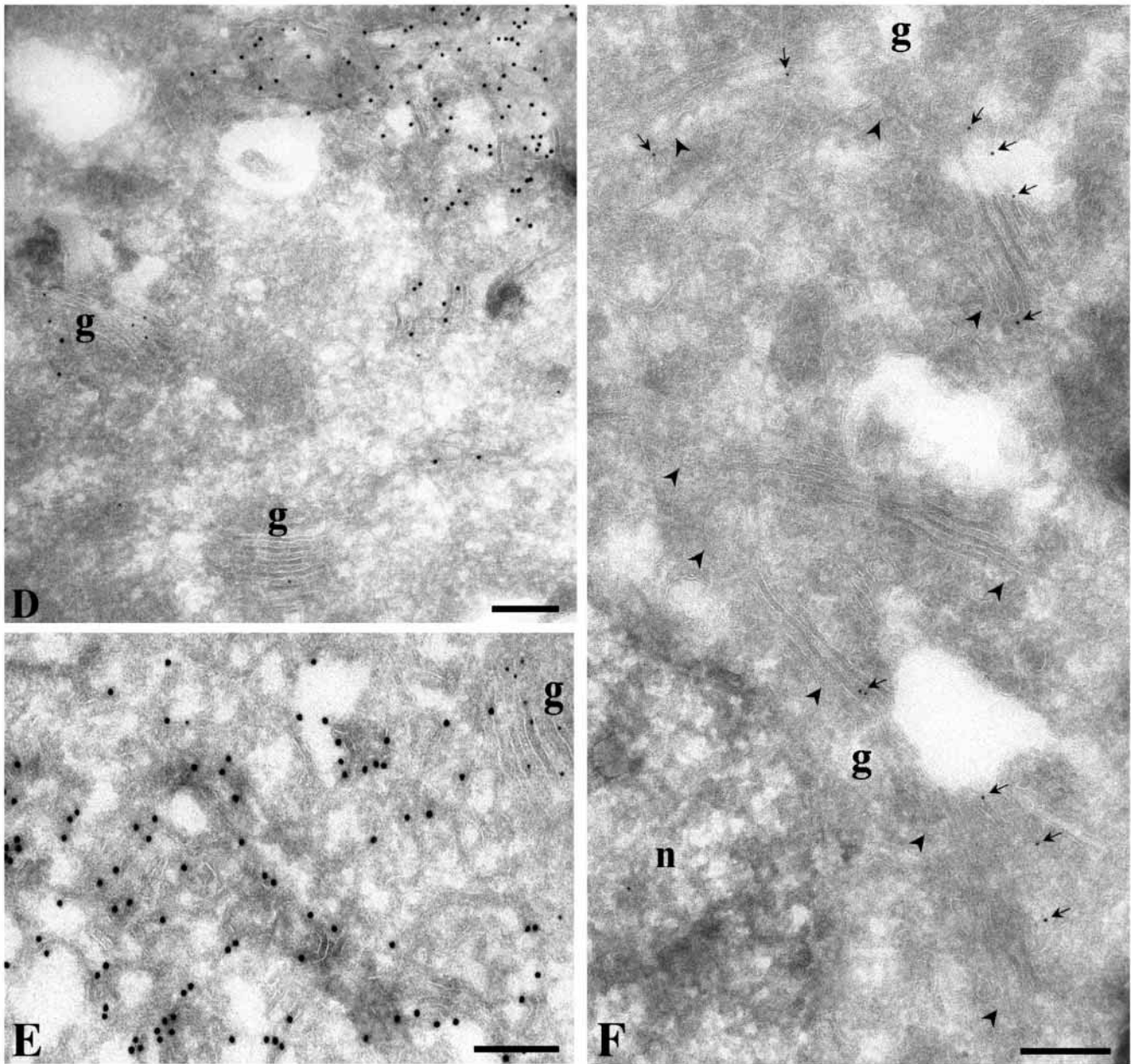
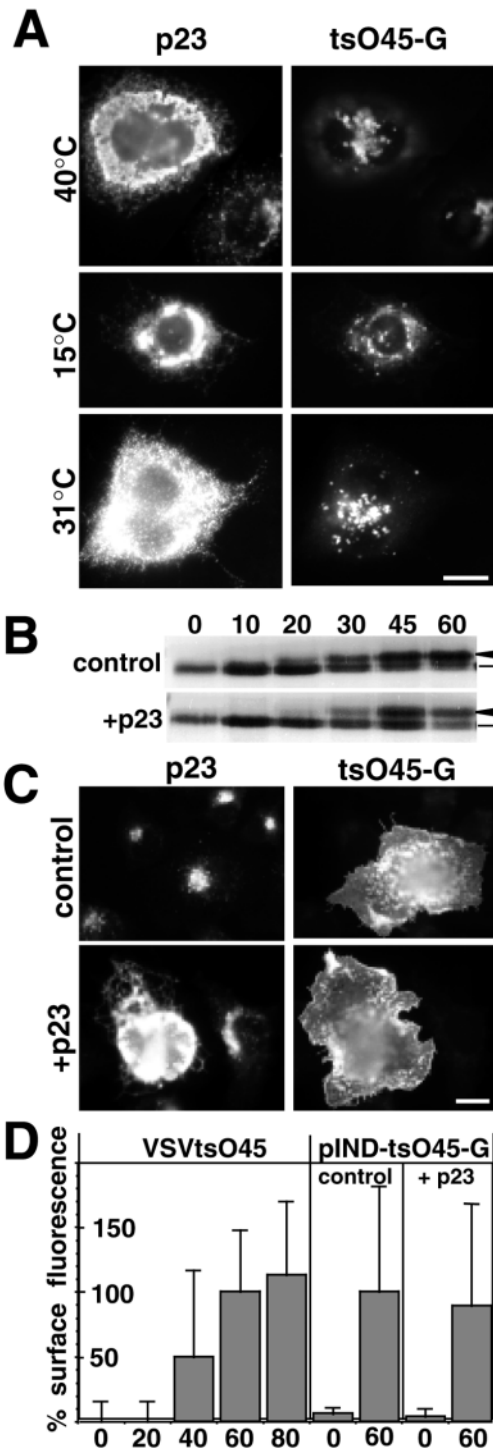


Fig. 4. The p23 protein is morphogenic; overexpression induces the formation of extensive tubulo-cisternal membranes. (A-C) Cells were infected with SFV-p23 in order to overexpress p23, and then processed for frozen sectioning using antibodies against p23, followed by 15 nm protein A-gold. (A-C) The resulting morphology of p23-labeled elements and Golgi membranes. The labeled elements comprise a large reticular structure in the perinuclear area of the cell. (A) A representative example from the centriolar region of the cell. Note the concentration of labeling in tubular profiles of 16-20 nm diameter (intralumenal distance, i.e. between inner surface of membranes). In some areas electron dense material is apparent on the cytoplasmic side of the membrane (double arrows). Note the constant luminal intermembrane distance (indicated by small arrowheads), and the higher electron-density of the lumen of the p23 membranes. This contrasts with the ER comprising the nuclear envelope in which the diameter is more irregular (large arrowheads, lower left) and which there is negligible labeling for p23. The p23 membranes are connected to p23-negative cisternal elements with more variable diameter (indicated by arrows) consistent with the p23 membranes being continuous with the ER. A small stack of cisternal elements, possibly a Golgi complex remnant (g) shows low labeling for p23. (B and C) Further examples of the p23-labeled elements and the uniformity of the membrane morphology (arrowheads). Note the extent of the labeled elements and their apparent complexity. (C) A slightly-extracted cell in which the morphology of the labeled tubular profiles is clearly evident and the labeling density is extremely high. (D-F) Cells were double-transfected with plasmids encoding for p23 and mycNAGT1-GFP (D-E), or single-transfected with mycNAGT1-GFP alone (F), and then processed for frozen sectioning using antibodies against p23 (D-E) or the myc epitope (D-F), followed by 15 nm (D-E) and 10 nm (D-F) protein A-gold, respectively. (D-E) Golgi stacks labeled with anti-myc antibodies (NAGT1, small gold) and membrane clusters (similar to those in A-C) labeled with anti-p23 antibodies (large gold). Note the high labeling for p23 in the tubular elements but not in the NAGT1-positive Golgi stacks (g). Also note that the Golgi stacks appear smaller in p23-transfected cells (D,E) than in the control cells transfected with NAGT1 alone (F; arrowheads indicate the extent of the cisternae; arrows indicate NAGT1 labeling). c, centriole; n, nucleus; m, mitochondria. Bars: 100 nm (A-D); 200 nm (E-F).



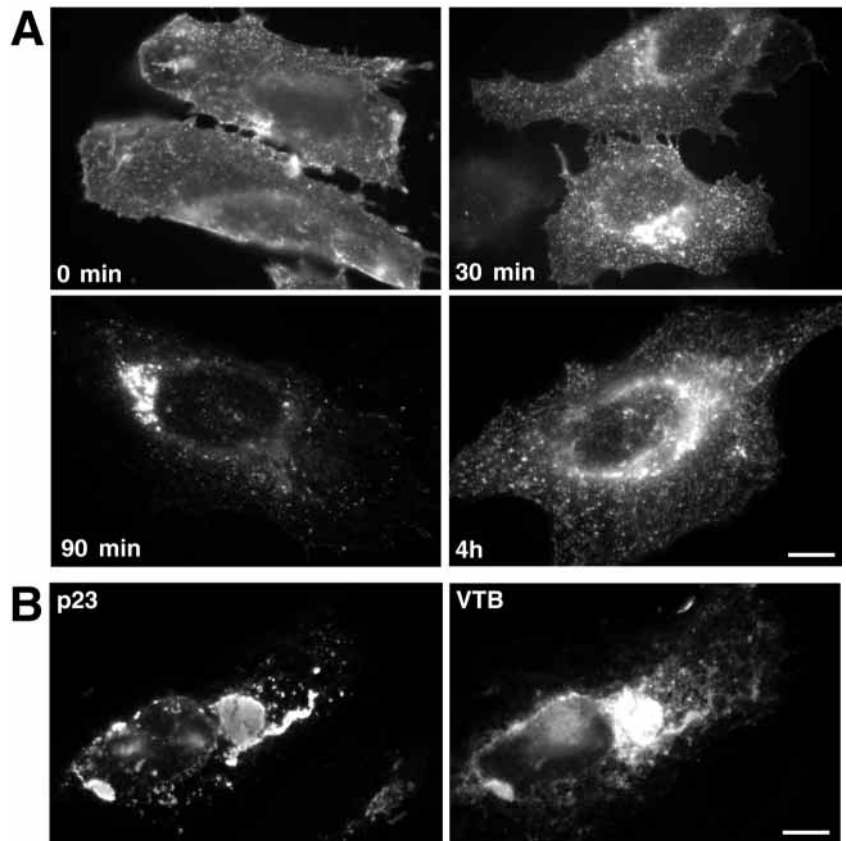
of ectopic p23 and relocalization of the endogenous protein may affect the integrity of the Golgi apparatus. Since such effects were difficult to study and quantify by electron microscopy, we studied the consequences of p23 overexpression and relocalization on the organization of the Golgi apparatus by a quantitative immunofluorescence analysis. It is important to note that morphological changes of the Golgi ribbon (e.g. the scattering of mini-stacks throughout the cytoplasm induced by microtubule depolymerization) are difficult to reveal by electron microscopy of thin sections but

Fig. 5. Anterograde transport of the transmembrane protein tsO45-G in cells that overexpress and relocalize p23. (A) BHK cells were co-infected with SFV-mycp23 and VSV-tsO45 at 40°C for 12 hours. After addition of cycloheximide, cells were further incubated at the indicated temperatures (40°C: no treatment; 15°C: 3 hours; 31°C: 30 minutes at 31°C), and processed for immunofluorescence. At 40°C, tsO45-G is retained in the ER, where it colocalizes with overexpressed p23. After shifting the temperature to 15°C or 31°C, tsO45-G is transported out of the ER to membranes of the intermediate compartment (15°C) or Golgi apparatus (31°C). (B,C) BHK cells were transfected with pIND-tsO45-G alone (control) or pIND-tsO45-G and pCB6-p23 (+p23), and 24 hours post-transfection tsO45-G expression was induced for 12 hours at 40°C. (B) Cells were pulsed with [³⁵S]methionine for 10 minutes. After addition of excess unlabelled methionine, cells were transferred to 31°C for the indicated times (minutes). The tsO45-G protein was immunoprecipitated and digested with endo H. Sensitive (line) and resistant (arrowhead) forms were separated by SDS-PAGE and revealed by autoradiography. Overexpression of p23 does not significantly alter the acquisition of endoH resistance. (C) Cycloheximide was added, the temperature was shifted to 31°C for 1 hour, and cells were fixed. Fixed cells were incubated with antibodies against tsO45-G, then permeabilized and incubated with antibodies against p23. The tsO45-G protein is transported to the plasma membrane both in control cells and in cells that overexpress exogenous p23. (D) BHK cells were infected with VSVtsO45 or transfected with pIND-tsO45-G. pIND-tsO45-G was transfected alone (control) or together with pCB6-p23 (+p23). Cells were incubated at 40°C for 3 hours after infection (VSVtsO45) or for 12 hours after induction of tsO45 expression (pINDtsO45). After addition of cycloheximide, temperature was shifted to 31°C for the indicated time (in minutes). Surface fluorescence of tsO45-G was quantified in ≥50 cells and expressed as % of the surface fluorescence after 60 minutes (100% = pIND-tsO45-G: control). Bars indicate the standard deviation. Overexpression and relocalization of p23 does not affect the transport of tsO45-G to the plasma membrane. The majority of tsO45-G molecules reach the plasma membrane 60 minutes after release of the temperature block (VSVtsO45), and thus, this time-window is well suited for these experiments (pIND-tsO45). Bars, 5 μm.

easily visualized by immunofluorescence of whole cells (e.g. Rogalski and Singer, 1984).

Here we used cells (HeLa), fixation conditions (methanol), and markers (see below) that easily reveal the membrane continuity of the Golgi ribbon in immunofluorescence. We used antibodies directed against giantin, a peripheral membrane protein of the Golgi (Linstedt and Hauri, 1993), and against two Golgi antigens (CTR 314 and CTR 433: Jasmin et al., 1989). In addition, we directly visualized the Golgi apparatus in a HeLa cell line (Shima et al., 1997) expressing a chimera of a green fluorescent protein (GFP) fused to the retention domain of *N*-acetylglucosaminyl-transferase (NAGTI). We observed that in a significant fraction of cells overexpressing p23 (≈35%; Fig. 7C), all these Golgi markers did not localize to a continuous and branched Golgi ribbon, but to smaller scattered elements (Fig. 7A). These scattered elements probably correspond in part to the Golgi mini-stacks, or perhaps to individual cisternae, observed by electron microscopy (Fig. 4A). Obviously, this approach may have underestimated the effects of p23 overexpression on Golgi structure, since only the segregation/fragmentation events that can be visualized within the two dimensions of the plane and within the limited resolution of light microscopy were

Fig. 6. Verotoxin B subunit (VTB) is transported from the plasma membrane to the ER. Overexpression and relocalization of p23 does not affect retrograde transport of VTB. HeLa cells were incubated with FITC-labeled VTB at 4°C, cells were then shifted to 37°C for the indicated times (A) or for 4 hours (B), and processed for immunofluorescence. (A) VTB binds to the plasma membrane (0 minutes; note the continuous labelling of cell edges and pseudopodia), is then transported to membranes of the perinuclear Golgi region (30 minutes, 90 minutes; note the gradual disappearance of plasma membrane labeling) and then reaches the ER (4 hours; note the absence of labelling on the cell edge). (B) After overexpression and relocalization of p23, VTB reaches ER-membranes and p23-clusters. VTB molecules labelled ER subdomains containing clusters of p23-molecules in a major proportion of transfected cells (72%, $n=25$).



considered. Nevertheless, these experiments confirmed that overexpression and relocalization of p23 induces important structural changes in the Golgi complex.

We concluded that these effects were primarily caused by the absence of p23 from CGN membranes, and not by retention and accumulation of an overexpressed protein in the ER. In order to confirm this, we performed control overexpression experiments with a myc-tagged version of the KDEL-receptor (mycERD2) cloned into the same expression vector (pCB6) as p23. The KDEL-receptor ERD2 colocalizes extensively with p23 in the CGN of control cells (Rojo et al., 1997b), and functions in the retrieval to the ER of soluble ER proteins that carry a c-terminal KDEL peptide (Lewis and Pelham, 1992). Upon overexpression, ERD2 distributes to the ER and induces the relocalization of Golgi proteins to the ER (Hsu et al., 1992). Here, overexpressed mycERD2 localized to the ER and induced the relocalization of Golgi proteins to the ER, but not the fragmentation of the Golgi ribbon (Fig. 7B). Interestingly, the effect of ERD2 overexpression was observed in a percentage of transfected cells (25-40%; Fig. 7C) similar to that observed in transfection experiments with mycp23 ($\approx 35\%$; Fig. 7C). Altogether, these results demonstrate that the presence of p23-domains in the CGN is necessary for the maintenance of normal Golgi morphology. Due to the morphogenic activity of clustered p23 molecules (Fig. 4), and its abundance in CGN membranes (Rojo et al., 1997b) we hypothesize that the p23 protein directly contributes to the acquisition and the maintenance of CGN-membrane morphology (large, flat, fenestrated cisternae).

DISCUSSION

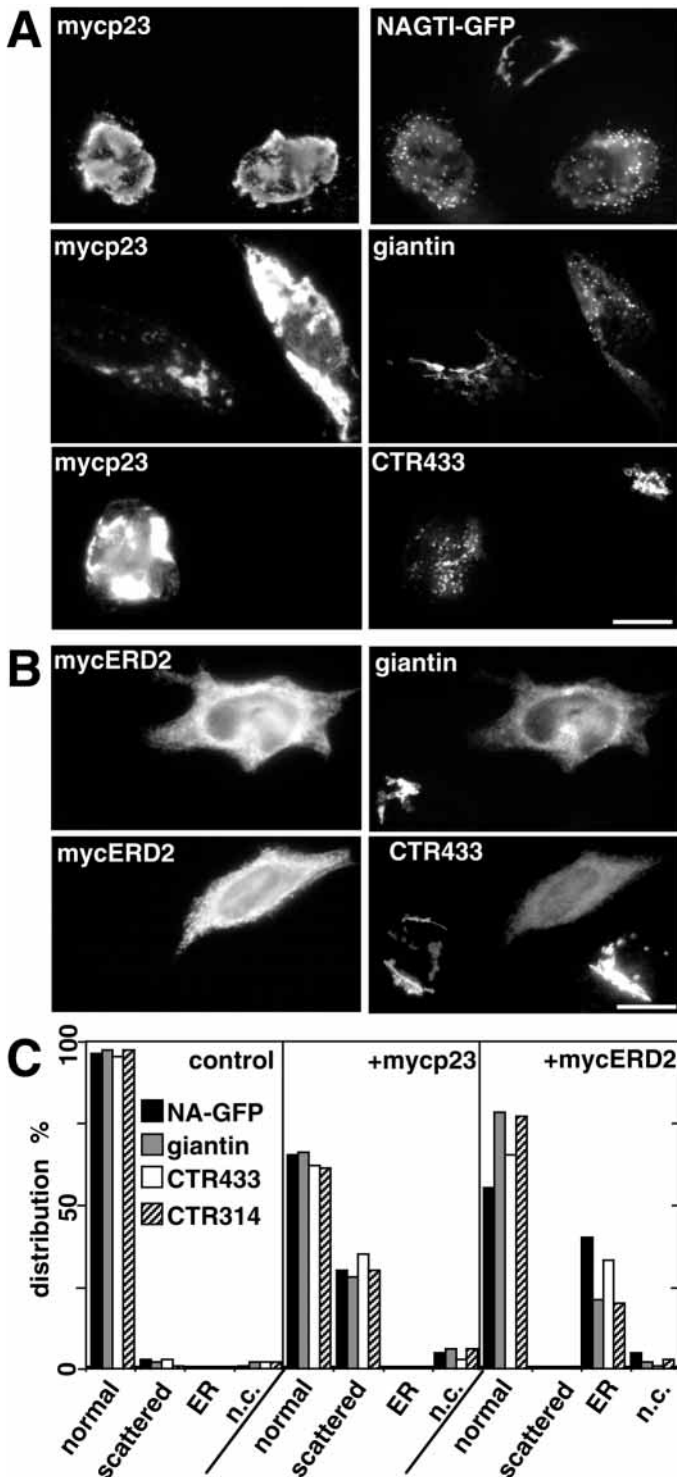
Here, we have expressed p23, a member of the p24 family, in mammalian cells. Exogenous p23 accumulated in the ER, where it induced the formation of specialized membrane domains with a characteristic and regular morphology. Expression of exogenous p23 also induced the relocalization of endogenous p23 from the CGN to the ER. Relocalization of

p23 did not affect transport of an anterograde or a retrograde cargo molecule, but led to changes in CGN and Golgi morphology. These results indicate that p23 is not directly involved in vesicular transport reactions, and that its morphogenic activity contributes to the generation and/or maintenance of CGN and Golgi morphology.

Overexpression and ER-retention of ectopically-expressed p23

In contrast to endogenous p23, which localizes to the CGN and to the intermediate compartment at steady state (Rojo et al., 1997b), overexpressed p23 was retained within specialized ER domains. Since two indicators of the unfolded protein response, BiP/grp78 and grp94, were not upregulated upon massive accumulation of p23, and since the oligomeric structure of endogenous and exogenous p23 was highly similar, we conclude that ER-retention of p23 was not due to p23-misfolding. This indicates that the steady state localization of endogenous p23 to the CGN does not solely rely on itself.

The behaviour of exogenous p23 is reminiscent of that of the Rubella virus E1 glycoprotein (RVE1-G): the properly folded RVE1-G is retained in the ER upon overexpression, where it induces a significant expansion of smooth ER membranes, with some resemblance to membranes containing ectopically expressed p23. However, upon coexpression of RVE1-G and RVE2-G, both proteins exit the ER (Hobman et al., 1992). Therefore, it is possible that exogenous p23 does not exit the ER because putative partners of p23, required for export, are titrated upon ectopic expression. These may include other members of the p24 family: recent studies have shown that p24 proteins can exit the ER when cDNAs for the



expression of 5 different p24 proteins are transfected into cells (Dominguez et al., 1998), and it was found that the putative yeast homologues of mammalian p23 and p24 (erv25p and emp24p) interact with each other in vivo (Belden and Barlowe, 1996). Blum and colleagues reported trafficking of exogenous, GFP-tagged p23 molecules beyond the ER (Blum et al., 1999), perhaps because the GFP-tag allowed the detection of much lower amounts of p23 molecules, when compared to those detected in this work. However, they also reported that GFP-

Fig. 7. Overexpression of p23 leads to fragmentation of the continuous Golgi ribbon. The indicated Golgi proteins were visualized after transfection of HeLa cells with mycp23 or mycERD2. (A) Overexpression of p23 (mycp23) leads to fragmentation of the Golgi ribbon. (B) Overexpression of the KDEL-receptor (mycERD2) leads to redistribution of Golgi proteins to the ER. (C) Quantitative analysis of the effect induced by overexpression of mycp23 and mycERD2 on Golgi structure. Randomly selected cells were inspected by immunofluorescence and classified according to the distribution of Golgi markers (NAGTI-GFP, giantin, CTR433, CTR314) into the following categories: normal, scattered, ER, or not fitting into any category (n.c.). For each condition (control, +mycp23, +mycERD2) cell counting was pursued until 1 category reached 100. Each category was then expressed as % of all counted cells. Overexpression of p23 leads to a fragmentation of the Golgi ribbon visible by immunofluorescence in $\approx 35\%$ of transfected cells. Overexpression of the KDEL-receptor leads to redistribution of Golgi proteins to the ER in 25–40% of transfected cells.

tagged p23 could cause the formation of large membranous structures.

Our data also show that endogenous p23 cycles between CGN and ER (Rojo et al., 1997b), and it is possible that ectopically expressed, properly folded p23 follows the same cycle (Jackson et al., 1993; Nickel et al., 1997; Blum et al., 1999). Yet, we failed to detect myc-p23 within CGN membranes, even when expressed at levels equal to those of endogenous p23 (see Fig. 1). Moreover, endogenous p23 is quantitatively relocated to ER-derived membranes containing ectopically expressed p23 or myc-p23. The simplest interpretation is that endogenous p23 continued cycling, and was 'trapped' by exogenous p23 when passing through the ER. Alternatively, it is possible that relocation is due to overexpression-induced alteration of the balance between anterograde and retrograde transport of p23. These observations strongly suggest (i) that endogenous and exogenous p23 interact with each other, and thus (ii) that the hypothetical interactions with other proteins cannot be of a permanent and/or stable nature. Indeed, if localization of the endogenous protein was conferred strictly by stable interactions with a partner protein, then this partner and p23 should be present in equal amounts. However, upon overexpression, exogenous p23 formed oligomers that were highly similar in size to endogenous p23. In addition, endogenous p23 is extremely abundant within CGN membranes (≈ 12500 copies/ μm^2 membrane surface area; Rojo et al., 1997b), far more than any known membrane protein of the CGN, or the Golgi complex.

Several anterograde and retrograde transport determinants have been identified on p24 proteins (Fiedler et al., 1996; Dominguez et al., 1998; Nakamura et al., 1998). Since cytoplasmic tails causing ER-retrieval can be masked via protein-protein interactions (Letourneur et al., 1995), it is possible that endogenous p23 exits the ER after its cytoplasmic tail has been masked by interaction with another (p24) protein. Therefore, it is conceivable that transport and localization of endogenous p23, and of other p24 proteins, are modulated by dynamic interactions that mask and/or expose such transport determinants.

A morphogenic function for the transmembrane protein p23

Numerous sorting and transport events occur in the

intermediate compartment and in the CGN (Teasdale and Jackson 1996; Kaiser and Ferro-Novick, 1998). The relocalization of endogenous p23 to the ER allowed us to investigate structure and function of these membranes after they had been depleted of p23.

It has been established that peptides equivalent to the cytoplasmic tail of p23 bind COPI and COPII *in vitro* (Sohn et al., 1996; Dominguez et al., 1998). We found that massive accumulation of p23 in ER-subdomains, and relocalization of endogenous p23 from the CGN to the ER did not affect the localization of COPI and COPII *in vivo*. In addition, we showed that, after BFA-mediated solubilization and reassociation, COPI associated to biosynthetic membranes apparently devoid of p23, but not to ER-membranes containing massive amounts of p23 (in agreement with similar studies on ERGIC-53: Vollenweider et al., 1998). It is likely that p23/p24 cytoplasmic tails interact with COPs *in vivo*, and mediate their loading on COP coated transport vesicles. However, the present work confirms that the cytoplasmic tail of p23 is not a major determinant for membrane binding of COPI (Rojo et al., 1997b). In agreement with this, COPI does not localize to the ER, where most transmembrane proteins with COPI-binding cytoplasmic tails reside (Teasdale and Jackson, 1996), but to the *cis* side of the Golgi (Oprins et al., 1993).

The relocalization of p23 did not affect transport of anterograde and retrograde cargo molecules to the plasma membrane, and somewhat delayed the acquisition of endoH resistance of tsO45-G. It is possible that minor changes in transport kinetics were not revealed when measuring ER to plasma membrane transport, or that a delay in ER to CGN transport (as revealed by acquisition of endo H resistance) did not affect transport between ER and plasma membrane. Alternatively, the slower processing of the glycodomain of tsO45 in the CGN may be due to disorganization of the CGN and of the Golgi ribbon, and not to slower transport between ER and Golgi. It is important to note that, in various systems, major morphological changes do not affect transport between different compartments of the biosynthetic pathway (Gahmberg et al., 1986; Sandoval and Carrasco, 1997). Altogether, these findings support the notion that p23 molecules do not directly participate in transport, and agree with our previous conclusions that antibodies against p23 tail inhibit transport because they alter CGN membrane dynamics (Rojo et al., 1997b). Two yeast members of the p24 family, emp24p and erv25p, are involved in protein sorting. The mechanism of action is not known, and two functional models have been proposed: (i) p24 proteins directly bind to cargo molecules on transient transport vesicles or (ii) p24 proteins ensure cargo loading through contributions to organelle structure (Schimmöller et al., 1995; Belden and Barlowe, 1996; Elrod-Erickson and Kaiser, 1996). The morphogenic role of p23 is compatible with a role of p24 proteins in cargo selection according to the second functional model.

Overexpression and ER-retention of exogenous p23 led to the generation of subdomains of the smooth ER that contained large amounts of p23. The ability to induce proliferation of smooth ER membranes is shared by other transmembrane proteins like the rubella virus E1 Glycoprotein (Hobman et al., 1992) and HMGCoA-reductase (Bergmann and Fusco, 1990). These p23-membranes were accessible to ER proteins (BiP, calnexin, misfolded VSV-G), and were devoid of other markers

of the CGN and of the Golgi apparatus. The morphology of these membranes (with a narrow and uniform luminal space) was different from ER cisternae (with a wider and variable intermembrane distance), and reminiscent of the CGN membranes where p23 localizes at steady state (Rojo et al., 1997b). In addition, the density of this ER-subdomain was similar to p23-membranes of the CGN. Despite their different properties, p23-membranes and the rough ER appeared continuous (at least dynamically). In this respect, it is important to note that membrane connections between different compartments of the early biosynthetic pathway have been reported (Lindsey and Ellisman, 1985; Krijnse-Locker et al., 1994).

Altogether, our data indicate that the morphology of p23-clusters in the smooth ER was determined by the abundant presence of p23 molecules. The p23 protein contains, like other p24 proteins, heptad repeats of hydrophobic aminoacids suited for coiled-coil interactions. Therefore, it is possible that size and morphology of these membranes results from extensive interactions and/or oligomerizations between p23 molecules. We had previously shown that p23 is a major component of the CGN, where it can make up to 30% of all integral membrane proteins, and we had proposed that p23 significantly contributes to the structure of this compartment (Rojo et al., 1997b). The potent morphogenic capacity of ectopically expressed p23 is fully consistent with a role of p23 in the morphology of the CGN.

Overexpression and relocalization of p23 led to the loss of normal Golgi morphology, resulting in the fragmentation of the continuous Golgi ribbon (as observed by immunofluorescence in $\approx 35\%$ of transfected cells), and in the appearance of smaller Golgi fragments, i.e. mini-stacks (as observed by electron microscopy). In agreement with our results, Blum et al. (1999) have also reported that GFP-tagged p23 and p24 molecules can alter the morphology of the Golgi complex upon overexpression. The Golgi apparatus can be disassembled during mitosis, and with agents (drugs and/or proteins) that mimic mitotic conditions or trigger exaggerated vesiculation and transport reactions (reviewed by Warren and Malhotra, 1998). In addition, the disappearance of the Golgi can be observed after relocalization of medial Golgi enzymes to the ER (Nilsson et al., 1994). The changes induced by p23 on Golgi structure did not appear to involve increased vesiculation and/or transport reactions, nor quantitative depletion of Golgi components. From this we conclude that the abundant presence of p23 in the CGN, and its morphogenic activity at this location, is required for normal Golgi morphology. At this stage, it is not known whether different p24 homologues (i) fulfill similar functions at different locations, (ii) display different functions at the same location, or (iii) act synergistically at the same compartment(s), but it is possible that other p24 proteins are also morphogenic. The presence of putative coiled-coil domains in p24 proteins at similar positions relative to the transmembrane domain enables heterotypic interactions between different p24 proteins (Emery et al., 1999). Therefore, p24 proteins may modulate organelle morphology via heterotypic interactions.

We gratefully acknowledge all the scientists who generously provided us with antibodies, cDNAs, and recombinant proteins (see Materials and Methods). We are indebted to Margaret Lindsay for her

expert assistance with immunolabeling experiments. We are also grateful to Marie-Hélène Beuchat and Majid Ghodousi for expert technical assistance and Gisou van der Goot for critical reading of the manuscript. This work was supported by grant no. 31-37296.93 from the Swiss National Science Foundation (to J. Gruenberg), grants from the National Health and Medical Research Council of Australia (to R.G. Parton), and grant RG 355/94 from the International Human Frontier Science Program (to J. Gruenberg and R. G. Parton).

REFERENCES

- Alcalde, J., Egea, G. and Sandoval, I. V. (1994). Gp74 – a membrane glycoprotein of the Cis-Golgi network that cycles through the endoplasmic reticulum and intermediate compartment. *J. Cell Biol.* **124**, 649-665.
- Balch, W. E., Elliott, M. M. and Keller, D. S. (1986). ATP-coupled transport of vesicular stomatitis virus G protein between the endoplasmic reticulum and the Golgi. *J. Biol. Chem.* **261**, 14681-14689.
- Belden, W. J. and Barlowe, C. (1996). Erv25p, a component of COPII-coated vesicles, forms a complex with emp24p that is required for efficient endoplasmic reticulum to Golgi transport. *J. Biol. Chem.* **271**, 26939-26946.
- Bergmann, J. E., Tokuyasu, K. T. and Singer, S. J. (1981). Passage of an integral membrane protein, the vesicular stomatitis virus glycoprotein, through the Golgi apparatus en route to the plasma membrane. *Proc. Nat. Acad. Sci. USA* **78**, 1746-1750.
- Bergmann, J. E. and Fusco P. J. (1990). The G protein of vesicular stomatitis virus has free access into and egress from the smooth endoplasmic reticulum of UT-1 cells. *J. Cell Biol.* **110**, 625-635.
- Blum, R., Pfeiffer, F., Feick, P., Nastainczyk, W., Kohler, B., Schafer, K. H. and Schulz, I. (1999). Intracellular localization and in vivo trafficking of p24A and p23. *J. Cell Sci.* **112**, 537-548.
- Brewer, C. B. (1994). Cytomegalovirus plasmid vectors for permanent lines of polarized epithelial cells. *Meth. Cell Biol.* **43**, 233-245.
- Burke, B., Griffiths, G., Reggio, H., Louvard, D. and Warren, G. (1982). A monoclonal antibody against a 135-K Golgi membrane protein. *EMBO J.* **12**, 1621-1628.
- Chen, C. and Okayama, H. (1987). High-efficiency transformation of mammalian cells by plasmid DNA. *Mol. Biol. Cell* **7**, 2745-2752.
- Cosson, P. and Letourneur, F. (1997). Coatamer (COPI)-coated vesicles: role in intracellular transport and protein sorting. *Curr. Opin. Cell Biol.* **9**, 484-487.
- Dominguez, M., Dejgaard, K., Fullekrug, J., Dahan, S., Fazel, A., Paccaud, J. P., Thomas, D. Y., Bergeron, J. J. and Nilsson, T. (1998). gp25L/emp24/p24 protein family members of the cis-Golgi network bind both COP I and II coatamer. *J. Cell Biol.* **140**, 751-765.
- Elrod-Erickson, M. J. and Kaiser, C. A. (1996). Genes that control the fidelity of endoplasmic reticulum to Golgi transport identified as suppressors of vesicle budding mutations. *Mol. Biol. Cell* **7**, 1043-1058.
- Emery, G., Gruenberg, J. and Rojo, M. (1999). The p24 family of small transmembrane proteins at the interface between endoplasmic reticulum and Golgi apparatus. *Protoplasma* **207**, 24-30.
- Evan, G. I., Lewis, G. K., Ramsay, G. and Bishop, J. M. (1985). Isolation of monoclonal antibodies specific for human c-myc proto-oncogene product. *Mol. Biol. Cell* **5**, 3610-3616.
- Fiedler, K., Veit, M., Stamnes, M. A. and Rothman, J. E. (1996). Bimodal interaction of coatamer with the p24 family of putative cargo receptors. *Science* **273**, 1396-1399.
- Fiedler, K. and Rothman, J. E. (1997). Sorting determinants in the transmembrane domain of p24 proteins. *J. Biol. Chem.* **272**, 24739-24742.
- Gahmberg, N., Pettersson, R. F. and Kaariainen, L. (1986). Efficient transport of Semliki Forest virus glycoproteins through a Golgi complex morphologically altered by Uukuniemi virus glycoproteins. *EMBO J.* **5**, 3111-3118.
- Gallione, C. J. and Rose, J. K. (1985). A single amino acid substitution in a hydrophobic domain causes temperature-sensitive cell-surface transport of a mutant viral glycoprotein. *J. Virol.* **54**, 374-382.
- Gayle, M. A., Slack, J. L., Bonnert, T. P., Renshaw, B. R., Sonoda, G., Taguchi, T., Testa, J. R., Dower, S. K. and Sims, J. E. (1996). Cloning of a putative ligand for the T1/ST2 receptor. *J. Biol. Chem.* **271**, 5784-5789.
- Griffiths, G., McDowall, A., Back, R. and Dubochet, J. (1984). On the preparation of cryosections for immunocytochemistry. *J. Ultrastruct. Res.* **89**, 65-78.
- Griffiths, G., Ericsson, M., Krijnselocker, J., Nilsson, T., Goud, B., Soling, H. D., Tang, B. L., Wong, S. H. and Hong, W. J. (1994). Localization of the lys, asp, glu, leu tetrapeptide receptor to the Golgi complex and the intermediate compartment in mammalian cells. *J. Cell Biol.* **127**, 1557-1574.
- Gruenberg, J. and Howell, K. E. (1985). Immuno-isolation of vesicles using antigenic sites either located on the cytoplasmic or the exoplasmic domain of an implanted viral protein. A quantitative analysis. *Eur. J. Cell Biol.* **38**, 312-321.
- Hammond, C. and Helenius, A. (1994). Quality control in the secretory pathway: retention of a misfolded viral membrane glycoprotein involves cycling between the ER, intermediate compartment, and Golgi apparatus. *J. Cell Biol.* **126**, 41-52.
- Hammond, C. and Helenius, A. (1995). Quality control in the secretory pathway. *Curr. Opin. Cell Biol.* **7**, 523-529.
- Hjelmeland, L. M. and Chrambach, A. (1984). Solubilization of functional membrane proteins. *Meth. Enzymol.* **104**, 305-328.
- Hobman, T. C., Woodward, L. and Farquhar, M. G. (1992). The rubella virus E1 glycoprotein is arrested in a novel post-ER, pre-Golgi compartment. *J. Cell Biol.* **118**, 795-811.
- Hsu, V. W., Shah, N. and Klausner, R. D. (1992). A brefeldin A-like phenotype is induced by the overexpression of a human ERD-2-like protein, ELP-1. *Cell* **69**, 625-635.
- Jackson, M. R., Nilsson, T. and Peterson, P. A. (1993). Retrieval of transmembrane proteins to the endoplasmic reticulum. *J. Cell Biol.* **121**, 317-333.
- Jasmin, B. J., Cartaud, J., Bornens, M. and Changeux, J. P. (1989). Golgi apparatus in chick skeletal muscle: changes in its distribution during end plate development and after denervation. *Proc. Nat. Acad. Sci. USA* **86**, 7218-7222.
- Johannes, L. and Goud, B. (1998). Surfing on a retrograde wave: how does Shiga toxin reach the endoplasmic reticulum? *Trends Cell Biol.* **8**, 158-162.
- Johannes, L., Tenza, D., Antony, C. and Goud, B. (1997). Retrograde transport of KDEL-bearing B-fragment of Shiga toxin. *J. Biol. Chem.* **272**, 19554-19561.
- Kaiser, C. and Ferro-Novick, S. (1998). Transport from the endoplasmic reticulum to the Golgi. *Curr. Opin. Cell Biol.* **10**, 477-482.
- Kim, J. H., Lingwood, C. A., Williams, D. B., Furuya, W., Manolson, M. F. and Grinstein, S. (1996). Dynamic measurement of the pH of the Golgi complex in living cells using retrograde transport of the verotoxin receptor. *J. Cell Biol.* **134**, 1387-1399.
- Kirchhausen, T., Bonifacino, J. S. and Riezman, H. (1997). Linking cargo to vesicle formation: receptor tail interactions with coat proteins. *Curr. Opin. Cell Biol.* **9**, 488-495.
- Kozutsumi, Y., Segal, M., Normington, K., Gething, M. J. and Sambrook, J. (1988). The presence of misfolded proteins in the endoplasmic reticulum signals the induction of glucose-regulated proteins. *Nature* **332**, 462-464.
- Kreis, T. E. (1986). Microinjected antibodies against the cytoplasmic domain of vesicular stomatitis virus glycoprotein block its transport to the cell surface. *EMBO J.* **5**, 931-941.
- Krijnselocker, J., Ericsson, M., Rottier, P. J. and Griffiths, G. (1994). Characterization of the budding compartment of mouse hepatitis virus: evidence that transport from the RER to the Golgi complex requires only one vesicular transport step. *J. Cell Biol.* **124**, 55-70.
- Kuehn, M. J. and Schekman, R. (1997). COPII and secretory cargo capture into transport vesicles. *Curr. Opin. Cell Biol.* **9**, 477-483.
- le Maire, M., Kwee, S., Andersen, J. P. and Moller, J. V. (1983). Mode of interaction of polyoxyethyleneglycol detergents with membrane proteins. *Eur. J. Biochem.* **129**, 525-532.
- le Maire, M., Aggerbeck, L. P., Monteilhet, C., Andersen, J. P. and Moller, J. V. (1986). The use of high-performance liquid chromatography for the determination of size and molecular weight of proteins: a caution and a list of membrane proteins suitable as standards. *Anal. Biochem.* **154**, 525-535.
- Letourneur, F., Hennecke, S., Demolliere, C. and Cosson, P. (1995). Steric masking of a dilysine endoplasmic reticulum retention motif during assembly of the human high affinity receptor for immunoglobulin E. *J. Cell Biol.* **129**, 971-978.
- Lewis, M. J. and Pelham, H. R. B. (1992). Ligand-induced redistribution of a human KDEL receptor from the Golgi complex to the endoplasmic reticulum. *Cell* **68**, 353-364.
- Liljestrom, P. and Garoff, H. (1991). A new generation of animal cell expression vectors based on the Semliki Forest virus replicon. *Biotechnology* **9**, 1356-1361.

- Lindsey, J. D. and Ellisman M. H.** (1985). The neuronal endomembrane system. I. Direct links between rough endoplasmic reticulum and the cis element of the Golgi apparatus. *J. Neurosci.* **5**, 3111-3123.
- Linstedt, A. D. and Hauri, H. P.** (1993). Giantin, a novel conserved Golgi membrane protein containing a cytoplasmic domain of at least 350 kDa. *Mol. Biol. Cell* **4**, 679-693.
- Liou, W., Geuze, H. J., Geelen, M. J. and Slot, J. W.** (1997). The autophagic and endocytic pathways converge at the nascent autophagic vacuoles. *J. Cell Biol* **136**, 61-70.
- Majoul, I., Sohn, K., Wieland, F. T., Pepperkok, R., Pizza, M., Hillemann, J. and Soling, H. D.** (1998). KDEL receptor (Erd2p)-mediated retrograde transport of the cholera toxin A subunit from the Golgi involves COPI, p23, and the COOH terminus of Erd2p. *J. Cell Biol.* **143**, 601-612.
- Nakamura, N., Yamazaki, S., Sato, K., Nakano, A., Sakaguchi, M. and Mihara, K.** (1998). Identification of potential regulatory elements for the transport of emp24p. *Mol. Biol. Cell* **9**, 3493-3503.
- Nickel, W., Sohn, K., Bunning, C. and Wieland, F. T.** (1997). p23, a major COPI-vesicle membrane protein, constitutively cycles through the early secretory pathway. *Proc. Nat. Acad. Sci. USA* **94**, 11393-11398.
- Nilsson, T., Hoe, M. H., Slusarewicz, P., Rabouille, C., Watson, R., Hunte, F., Watzel, G., Berger, E. G. and Warren, G.** (1994). Kin recognition between medial Golgi enzymes in HeLa cells. *EMBO J.* **13**, 562-574.
- Oprins, A., Duden, R., Kreis, T. E., Geuze, H. J. and Slot, J. W.** (1993). b-COP localizes mainly to the *cis*-Golgi side in exocrine pancreas. *J. Cell Biol.* **121**, 49-59.
- Orci, L., Palmer, D. J., Ravazzola, M., Perrelet, A., Amherdt, M. and Rothman, J. E.** (1993). Budding from Golgi membranes requires the coatamer complex of non-clathrin coat proteins. *Nature* **362**, 648-652.
- Rogalski, A. A. and Singer, S. J.** (1984). Associations of elements of the Golgi apparatus with microtubules. *J. Cell Biol.* **99**, 1092-1100.
- Rojo, M.** (1993). Studies on the interaction of mitochondrial creatine kinase with membranes and structural studies on the adenine nucleotide translocator. Ph.D. thesis 10042 ETH Zürich, Switzerland.
- Rojo, M. and Wallimann, T.** (1994). The mitochondrial ATP/ADP carrier: interaction with detergents and purification by a novel procedure. *Biochim. Biophys. Acta* **1187**, 360-367.
- Rojo, M., Budin, N., Kellner, R. and Gruenberg, J.** (1997a). Generation of proteoliposomes from subcellular fractions. *Electrophoresis* **18**, 2620-2628.
- Rojo, M., Pepperkok, R., Emery, G., Kellner, R., Stang, E., Parton, R. G. and Gruenberg, J.** (1997b). Involvement of the transmembrane protein p23 in biosynthetic protein transport. *J. Cell Biol.* **139**, 1119-1135.
- Sandoval, I. V. and Carrasco, L.** (1997). Poliovirus infection and expression of the poliovirus protein 2B provoke the disassembly of the Golgi complex, the organelle target for the antipoliovirus drug Ro-090179. *J. Virol.* **71**, 4679-4693.
- Schimmöller, F., Singerkruger, B., Schroder, S., Kruger, U., Barlowe, C. and Riezman, H.** (1995). The absence of emp24p, a component of ER-derived COPII-coated vesicles, causes a defect in transport of selected proteins to the Golgi. *EMBO J.* **14**, 1329-1339.
- Shima, D. T., Haldar, K., Pepperkok, R., Watson, R. and Warren, G.** (1997). Partitioning of the Golgi apparatus during mitosis in living HeLa cells. *J. Cell Biol.* **137**, 1211-1228.
- Sohn, K., Orci, L., Ravazzola, M., Amherdt, M., Bremser, M., Lottspeich, F., Fiedler, K., Helms, J. B. and Wieland, F. T.** (1996). A major transmembrane protein of Golgi-derived COPI-coated vesicles involved in coatamer binding. *J. Cell Biol.* **135**, 1239-1248.
- Stamnes, M. A., Craighead, M. W., Hoe, M. H., Lampen, N., Geromanos, S., Tempst, P. and Rothman, J. E.** (1995). An integral membrane component of coatamer-coated transport vesicles defines a family of proteins involved in budding. *Proc. Nat. Acad. Sci. USA* **92**, 8011-8015.
- Tang, B. L., Peter, F., Krijnse-Locker, J., Low, S. H., Griffiths, G. and Hong, W.** (1997). The mammalian homolog of yeast Sec13p is enriched in the intermediate compartment and is essential for protein transport from the endoplasmic reticulum to the Golgi apparatus. *Mol. Biol. Cell* **17**, 256-266.
- Teasdale, R. D. and Jackson, M. R.** (1996). Signal-mediated sorting of membrane proteins between the endoplasmic reticulum and the Golgi apparatus. *Annu. Rev. Cell Dev. Biol.* **12**, 27-54.
- Wessel, D. and Flügge, U. J.** (1984). A method for the quantitative recovery of protein in dilute solution in the presence of detergents and lipids. *Anal. Biochem.* **138**, 141-143.
- Vollenweider, F., Kappeler, F., Itin, C. and Hauri, H. P.** (1998). Mistargeting of the lectin ERGIC-53 to the endoplasmic reticulum of HeLa cells impairs the secretion of a lysosomal enzyme. *J. Cell Biol.* **142**, 377-389.
- Warren, G. and Malhotra, V.** (1998). The organisation of the Golgi apparatus. *Curr. Opin. Cell Biol.* **10**, 493-498.
- Zulauf, M., Weckström, K., Hayter, J. B., Degiorgio, V. and Corti, M.** (1985). Neutron scattering study of micelle structure in isotropic aqueous solutions of poly(oxyethylene) amphiphiles. *J. Phys. Chem.* **89**, 3411-3417.